where the symbol $*^{T}$ denotes the transpose of a matrix. To put it alternatively, the diagonal elements of [S] dictate the symmetry of the network, while the off-diagonal ones, the reciprocity of it. For the sake of completeness, we note that the passivity of the medium is determined by the negativeness of the matrix $\frac{[\epsilon_r]-[\epsilon_r]^{CT}}{2j}$, where the operator $*^{CT}$ corresponds to the conjugate transpose of a matrix. By comparing the complex values of certain elements from matrix [S], we realized that the component which is parallel to the incident field remains the same regardless of the side that is excited. More specifically, we obtain the equalities:

$$S_{21}^{xx}=S_{12}^{xx}, \quad S_{21}^{yy}=S_{12}^{yy} \tag{6}$$

for arbitrary combination of the parameters (ϵ_{rxx}, ϵ_{rxy}, ϵ_{ryx}, ϵ_{ryy}). For this reason, to evaluate the nonreciprocity of the effective medium, we focus on the other four pairs of the off-diagonal elements of matrix [S], and we define the following difference quantities normalized to unity:

$$\begin{aligned} DS_{11}&=\frac{|S_{11}^{xx}-S_{11}^{xy}|}{|S_{11}^{yx}|+|S_{11}^{xy}|}, DS_{12}=\frac{|S_{12}^{xy}-S_{21}^{yx}|}{|S_{12}^{xy}|+|S_{21}^{yx}|}, \\ DS_{21}&=\frac{|S_{21}^{xy}-S_{12}^{yx}|}{|S_{21}^{xy}|+|S_{12}^{yx}|}, DS_{22}=\frac{|S_{22}^{yx}-S_{22}^{xy}|}{|S_{22}^{yx}|+|S_{22}^{xy}|}. \end{aligned} \tag{7}$$

What is most impressive is that the variations of the aforementioned four quantities (DS_{11}, DS_{12}, DS_{21}, DS_{22}) are numerically equal to each other, with respect to arbitrary selection of the relative permittivities (ϵ_{rxx}, ϵ_{rxy}, ϵ_{ryx}, ϵ_{ryy}). As a result, the degree of nonreciprocity of the medium is solely expressed by one positive quantity DS varying between 0 and 1:

$$0=\mathrm{NRI}=DS_{11}=DS_{12}=DS_{21}=DS_{22}<1, \tag{8}$$

which we call "nonreciprocity index" NRI. Obviously, for NRI = 0, we have a reciprocal medium and in case NRI $\rightarrow$ 1, giant nonreciprocity is occurred.

4. NUMERICAL RESULTS

Through extensive numerical simulations, we concluded that the function NRI possesses the following properties: (i) It is independent from the electrical (and the physical) thickness of the slab which is natural, since the nonreciprocity is not related to the size of the layer. (ii) It is numerically independent from the diagonal permittivities (ϵ_{rxx}, ϵ_{ryy}) of the matrix [ϵ_r], because they are related to the symmetry and not to the reciprocity of the device. (iii) The contour levels of NRI with respect to ($\Re[\in_{ryx}], \Im[\in_{ryx}]$) are dependent basically on the magnitude of the other off-diagonal component $|\epsilon_{rxy}|$. (iv) The dependence of NRI on the argument θ of ϵ_{rxy} is trivial; in particular, the two-dimensional distribution for an arbitrary ϵ_{rxy} with magnitude $|\epsilon_{rxy}|$ and argument θ is formulated as a rotation of the corresponding one for real positive $\epsilon_{rxy}=|\epsilon_{rxy}|$ ($\theta=0$) by the angle θ.

For these reasons, we represent (Fig. 3) the contour plots of NRI with respect to ($\Re[\in_{ryx}], \Im[\in_{ryx}]$) for various magnitudes $|\epsilon_{rxy}|$ with $\theta=0$. By inspection of the graphs, one can clearly notice that NRI = 0 when $\epsilon_{rxy}=\epsilon_{ryx}$ and far from this point, the depicted quantity gets increased (and restored at NRI = 0:9) with more rapid pace, the smaller is the magnitude $|\epsilon_{rxy}|$. Furthermore, the isocontour surfaces are symmetric with respect to the line $\arg(\epsilon_{ryx})=\theta$. The shortest path on the considered map in order to reach the maximal nonreciprocity index NRI is to follow the line $\arg(\epsilon_{ryx})=\theta$ toward the origin. In other words, a specific asymmetry of [S] with the minimum asymmetry of [ϵ_r] is achieved when ϵ_{ryx} possesses magnitudes very close to zero.

REFERENCES

1. Y. Ayasli, Non-ferrite, non-reciprocal phase shifter and circulator, US Patent, 4801901, 1989.
2. D. Sounas, C. Caloz, and A. Alu, Giant non-reciprocity at the subwavelength scale using angular momentum-biased metamaterials, Nat Commun 4 (2013), 2407.
3. K. Nishimura, Nonreciprocity of electromagnetic wave propagation characteristics in a grounded ferrite slab waveguide with a metallic strip grating, In: Proceedings of the 39th European Microwave Conference, Rome, Italy, 2009, pp. 727–730.
4. C.L. Hogan, The microwave gyrator, Bell Syst Tech J 31 (1952), 1–31.
5. A.G. Fox, S.E. Miller, and M.T. Weiss, Behavior and applications of ferrites in the microwave region, Bell Syst Tech J 34 (1954), 1–31.
6. Philips semiconductors, circulators and isolators, unique passive devices application notes, 98035.
7. C. Wenzel, Low frequency circulator/isolator uses no ferrite or magnet, RF Design, 1991.
8. D. G. Hoag, Electromagnetic isolator/actuator system, US Patent, 4849666, 1989.
9. H. Lira, Z. Yu, S. Fan, and M. Lipson, Electrically driven nonreciprocity induced by interband photonic transition on a silicon chip, Phys Rev Lett 109 (2102), 033901.
10. D. Sounas and C. Caloz, Electromagnetic nonreciprocity and gyrotropy of graphene, Appl Phys Lett 98 (2011), 021911.
11. C. He, X.-C. Sun, Z. Zhang, C.-S. Yuan, M.-H. Lu, Y.-F. Chen, and C. Sun, Nonreciprocal resonant transmission/reflection based on a one-dimensional photonic crystal adjacent to the magneto-optical metal film, Opt Express 21 (2013), 28934.
12. Y. Leviatan and G.S. Sheaffer, Analysis of inductive dielectric posts in rectangular waveguide, IEEE Trans Microwave Theory Tech 35 (1987), 48–59.

IMPLEMENTATION OF CROSS COUPLINGS IN MICROWAVE BANDPASS FILTERS

B. A. Belyaev[1,2,3], A. M. Serzhantov[1,2], Y. F. Bal'va[1,3], V. V. Tyurnev[1,2], A. A. Leksikov[1,2,3], and R. G. Galeev[4]

[1] Kirensky Institute of Physics, Siberian Branch, Russian Academy of Sciences, Krasnoyarsk, Russia; Corresponding author: belyaev@iph.krasn.ru

[2] Institute of Engineering Physics and Radio Electronics, Siberian Federal University, Krasnoyarsk, Russia

[3] Reshetnev Siberian State Aerospace University, Krasnoyarsk, Russia

[4] OJSC Scientific Production Enterprise "Radiosviaz", Krasnoyarsk, Russia

Received 16 January 2014

ABSTRACT: *New quasi-lumped resonator bandpass filters with cross couplings are presented. Coaxial and suspended stripline structures are considered. These filters are notable for their extremely wide and deep upper stopbands at small dimensions. They also have transmission zeros near the passband that significantly improve frequency selectivity. Photographs and measured frequency responses for the four fabricated filters are presented.* © 2014 Wiley Periodicals, Inc. Microwave Opt Technol Lett 56:2021–2025, 2014; View this article online at wileyonlinelibrary.com. DOI 10.1002/mop.28507

Key words: *microwave filters; elliptic-function bandpass filters; transmission zeros; cross couplings*

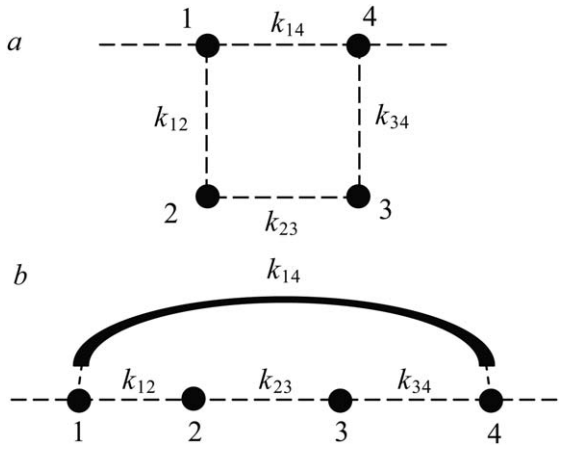

Figure 1 Direct (a) and indirect (b) cross couplings in the resonator quadruplet

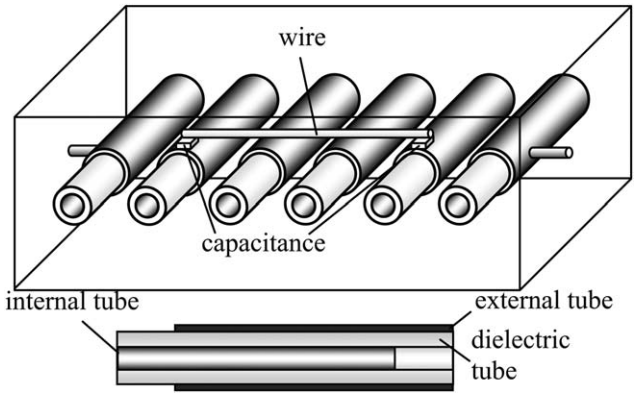

Figure 2 Layout of the coaxial filter No. 1

1. INTRODUCTION

Elliptic-function bandpass filters are known for their high selectivity. They have transmission zeros in stopbands, which significantly improve frequency responses of the filters. One of the ways to realize transmission zeros is the arrangement of additional signal paths in the filter by means of additional couplings between nonadjacent resonators (i.e., cross couplings). A transmission zero arises when the signals passing the two parallel paths have the same amplitudes and opposite phases. Various constructions of the cross-coupled microstrip filters are described in the monograph [1]. Trisection and quadruplet coupling topologies are well-known. These topologies are good for cascading to obtain the higher order frequency response with more number of transmission zeros.

Every trisection stage in the cascaded filter generates only one transmission zero. Its frequency is situated below or above the passband depending on the type of the cross coupling (i.e., sign of k_{13}) between the first and third resonators. At that, the stronger the cross coupling, the closer to the passband the transmission zero situates.

Every quadruplet stage generates none or two transmission zeros. They arise if the sign of the cross-coupling coefficient k_{14} between the first and fourth resonators is opposite to the sign of the product of all nearest coupling coefficients $k_{12}k_{23}k_{34}$. Two transmission zeros situate symmetrically on both sides of the passband if the frequency dispersion of all the coupling coefficients k_{ij} is not too strong near the passband. They also move closer to the passband when the cross coupling (k_{14}) is made stronger. In case of a strong frequency dispersion of k_{14}, the transmission zeros may be both situated below or above the passband if k_{14} inverts its sign near the passband.

The cross coupling in most conventional designs of the cross-coupled filters is direct, that is, it is fulfilled without the use of a complementary coupling element between nonadjacent resonators [Fig. 1(a)]. The direct cross coupling is frequently made with inductive or capacitive iris in the metal wall of the waveguide [2,3] or coaxial filters [4]. As for planar filters, the cross-coupled resonators often have a common section of coupled transmission lines [1]. The direct cross coupling implementation is complicated and such filters are difficult to tune. When the distance between the nonadjacent resonators is too long to ensure the required cross coupling, designers use complementary pins, or transmission line sections [5,6]. Such cross coupling is indirect [Fig. 1(b)].

In this letter, we present some new constructions of the highly selective cross-coupled bandpass filters where the cross coupling is implemented with a complementary nonresonant transmission line section.

2. QUASI-LUMPED COAXIAL FILTER

A new quasi-lumped resonator was recently proposed [7]. It consists of two coaxial tubular conductors each of them is grounded by one of its ends to the metal case. It differs in high ratio of the resonant frequencies for the first spurious mode and the fundamental mode. It also differs in small size and high quality factor. The frequency responses of the cross-coupling free bandpass filters of the forth order were studied in Refs. 8,9.

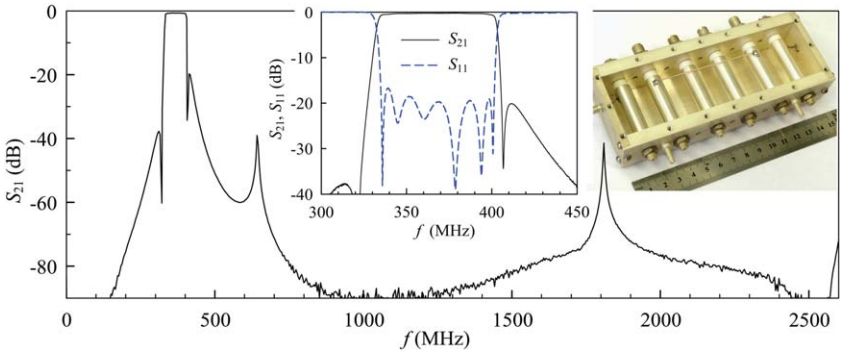

Figure 3 Measured frequency response of filter No. 1. [Color figure can be viewed in the online issue, which is available at wileyonlinelibrary.com]

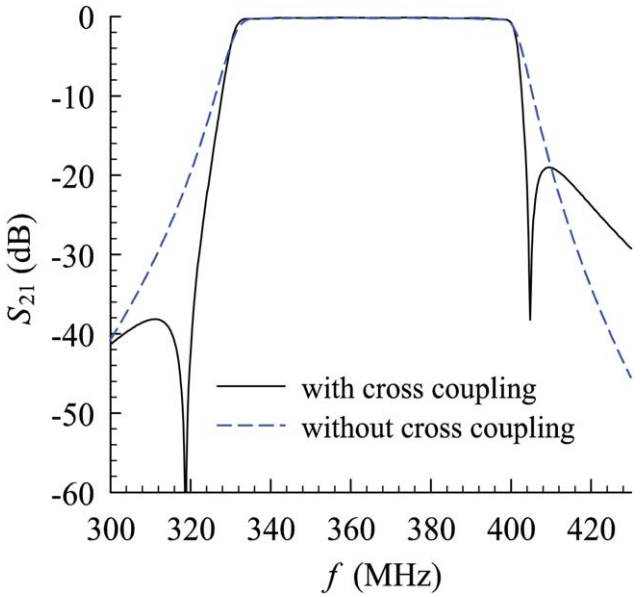

Figure 4 Frequency responses of filter No. 1 with and without cross coupling. [Color figure can be viewed in the online issue, which is available at wileyonlinelibrary.com]

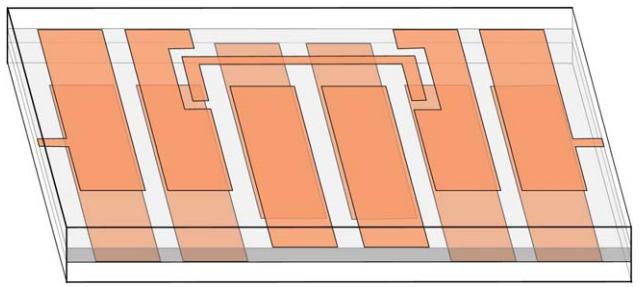

Figure 5 Layout of the suspended stripline filter No. 2. [Color figure can be viewed in the online issue, which is available at wileyonlinelibrary.com]

An example of an indirect cross coupling implemented in the quasi-lumped coaxial filter is shown in Figure 2. Filter No. 1 has a row of six EM-coupled coaxial resonators where inductive (positive) couplings prevail over corresponding capacitive (negative) ones. Here the coaxial tubular conductors in every resonator are insulated by a polytetrafluoroethylene pipe (ε_r=2.1). Note that the resonators in the filter are very short. Their relative length $l_r/\lambda = 0.054$ where l_r is the resonator length and λ is wavelength in free space at the resonant frequency. The first and the sixth resonators are tapped to the filter ports. The second and the fifth resonators have a cross coupling that is implemented with the use of a piece of insulated wire and two capacitors mounted on the resonators (Fig. 2). This means that the cross-coupling coefficient k_{25} is negative. The filter case has the inner dimensions of 143 × 44 × 31 mm^3.

Filter No. 1 and all other filters that are presented below were manually designed using a 3D EM simulator and a special optimization method based on universal physical rules [10,11]. We did not use equivalent circuits, coupling coefficients, and coupling matrices during the filter design.

Figure 3 shows the photograph and the measured frequency response of the fabricated coaxial filter. The passband has the center frequency f_0=368 MHz, the 3-dB bandwidth $\Delta f = 70$ MHz (19%), the minimum insertion loss $L = 0.23$ dB, and the minimum return loss $R = 17$ dB. Besides two transmission zeros at the frequencies $f_{z1} = 321$ MHz and $f_{z2} = 407$ MHz, the cross coupling generates a series of spurious transmission peaks at all resonant frequencies of the wire ensuring the cross coupling. Two first peaks of −42 and −41 dB are situated at the frequencies f_{p1}=642 MHz and f_{p2}=1810 MHz, respectively.

Figure 4 shows the simulated frequency responses of filter No. 1 in the presence and absence of the cross coupling. The filters in both cases were synthesized for the same passband as the passband of the frequency response in Figure 3. The solid line in Figure 4 refers to the filter with the cross coupling, and the dash line refers to the filter without that. Similarly, simulated frequency responses were obtained for all other filters that are presented below.

3. STRIPLINE FILTERS ON SINGLE-LAYER SUSPENDED SUBSTRATE

A new quasi-lumped suspended stripline resonator was proposed in [12]. This resonator has the same advantages as the quasi-lumped coaxial resonator. It consists of two strip conductors oppositely placed on both sides of a single-layer dielectric substrate that is suspended inside a metal case. Both strip conductors are grounded by one end in each of the conductors to the opposite walls of the metal case. The frequency responses of the cross-coupling free suspended stripline bandpass filters were studied in [12]. The study of similar filters but filled with

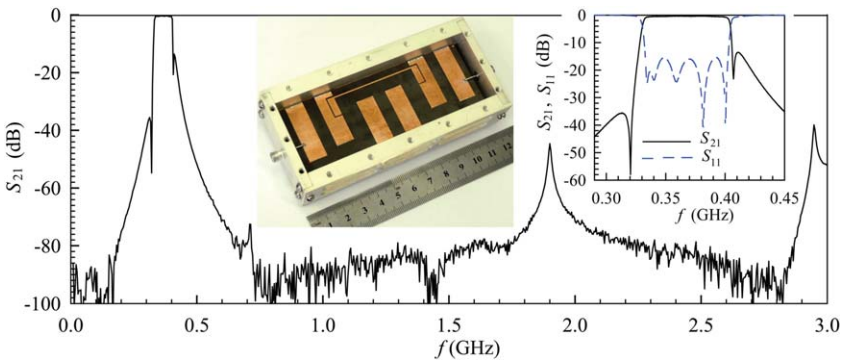

Figure 6 Measured frequency response of filter No. 2. [Color figure can be viewed in the online issue, which is available at wileyonlinelibrary.com]

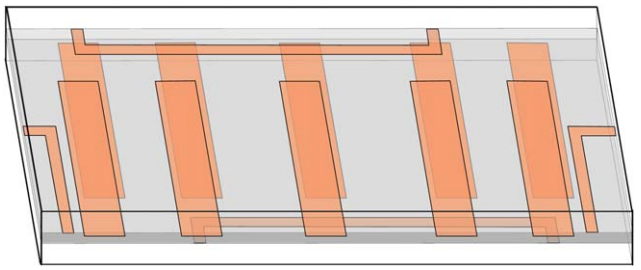

Figure 7 Layout of the suspended stripline filter No. 3. [Color figure can be viewed in the online issue, which is available at wileyonlinelibrary.com]

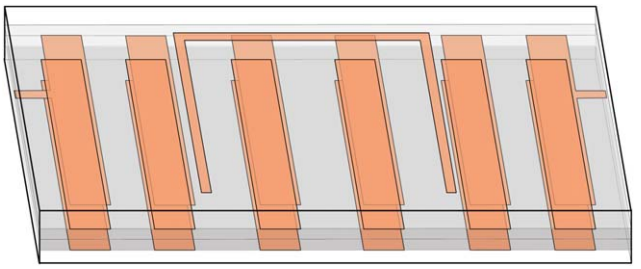

Figure 9 Layout of the suspended stripline filter No. 4. [Color figure can be viewed in the online issue, which is available at wileyonlinelibrary.com]

homogeneous dielectric and realized with the use of LTCC technology was presented in [13].

An implementation example of an indirect cross coupling in the quasi-lumped suspended stripline filter is shown in Figure 5. Filter No. 2 has a metal case with inner dimensions of 100 × 40 × 24 mm^3. The single-layer substrate of filter No. 2 is made of FAF-4D (foil-coated reinforced polytetrafluoroethylene sheet) with the thickness $h_d = 0.5$ mm and permittivity $\varepsilon_r \approx 2.5$. The filter has six EM-coupled suspended stripline resonators where inductive couplings prevail over corresponding capacitive ones. This means that all the coupling coefficients between the nearest resonators are positive. All the strip conductors in the resonators have the length $l_s = 35$ mm. All the resonators have the relative length $l_r/\lambda = 0.049$. The first and sixth resonators are tapped to the filter ports. The second and the fifth resonators have a cross coupling that is implemented with the use of a narrow strip conductor terminated by rectangular electrodes. Each of the electrodes together with the resonator strip conductor on opposite surface of the substrate forms a capacitor. Thus, the indirect cross coupling between the second and fifth resonators is capacitive (i.e., $k_{25}<0$).

Figure 6 shows the photograph and the measured frequency response of the fabricated suspended stripline filter No. 2. Its passband has the center frequency $f_0 = 369$ MHz, the 3-dB bandwidth $\Delta f = 75$ MHz (20%), the minimum insertion loss $L = 0.35$ dB, and the minimum return loss $R = 15.4$ dB. Besides two transmission zeros at the frequencies $f_{z1} = 321$ MHz and $f_{z2} = 407$ MHz, the cross coupling generates a series of spurious transmission peaks at all its resonant frequencies. Three first peaks of −73, −45, and −38 dB are situated at the frequencies $f_{p1} = 714$ MHz, $f_{p2} = 1900$ MHz, and $f_{p3} = 2948$ MHz, respectively.

Another implementation example of the indirect cross coupling in the quasi-lumped suspended stripline filter is shown in Figure 7. Filter No. 3 has a row of five EM-coupled resonators where inductive (positive) couplings prevail over corresponding capacitive (negative) ones. The filter substrate is made of ceramics barium-niobium-strontium titanate with $\varepsilon_r \approx 80$. It has the thickness $h_d = 1$ mm. The metal case of the filter has the inner dimensions of 44 × 5.5 × 6 mm^3. The first and fifth resonators are inductively coupled with the filter ports. Each of suspended stripline resonators has the relative length $l_r/\lambda = 0.026$.

Filter No. 3 has two cross couplings and they are symmetrical. Every coupling is implemented with the use of a narrow Π-shaped strip conductor. The first coupling is arranged between the first and fourth resonators, and its conductor is placed on one substrate surface. The second coupling is arranged between the second and fifth resonators, and its conductor is placed on the opposite substrate surface.

Both conductor ends in every cross coupling are connected to the metal case walls making the cross coupling inductive. However, the cross-coupling coefficients k_{14} and k_{25} are negative because the Π-shaped conductor is rather long for its resonant frequencies f_1 and f_2 to satisfy the inequality $f_1 < f_0 < f_2$, that is, the currents in both conductor ends flow in opposite directions near the center frequency f_0. The Π-shaped conductors in narrowband filters turn out to be electrically long when their suspended substrate has very high permittivity ε_r.

Figure 8 shows the photograph and the measured frequency response of the fabricated filter No. 3. Its passband has the center frequency $f_0 = 1.415$ GHz, the 3-dB bandwidth $\Delta f = 28$ MHz (2%), the minimum insertion loss $L = 4.35$ dB, and the minimum return loss $R = 14$ dB. Besides two transmission zeros at the frequencies $f_{z1} = 1.368$ GHz and $f_{z2} = 1.458$ GHz, the cross couplings generate a series of spurious transmission peaks at all

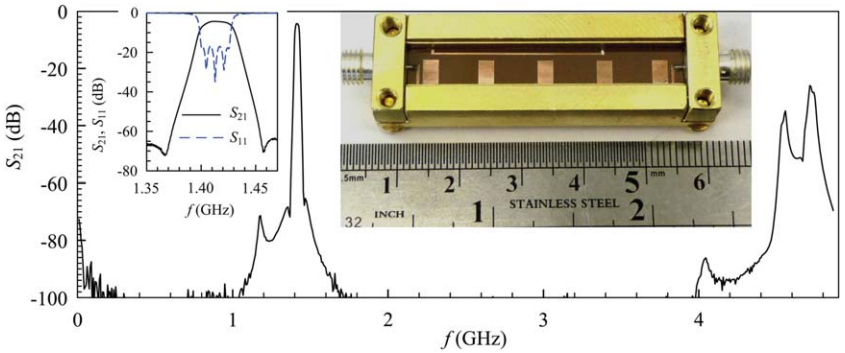

Figure 8 Measured frequency response of filter No. 3. [Color figure can be viewed in the online issue, which is available at wileyonlinelibrary.com]